Visible microdisk and photonic crystals lasers based on InGaP/InGaAlP system

Zhaoyu Zhang, Lan Yang, Victor Liu, Ting Hong, Kerry Vahala, et al.

SPIE.

Visible microdisk and photonic crystals lasers based on InGaP/InGaAlP system

Zhaoyu Zhang[1], Lan Yang[2], Victor Liu[1], Ting Hong[2], Kerry Vahala[2] and Axel Scherer[1,2]

1. Department of Electrical Engineering, California Institute of Technology, Pasadena, CA91125
2. Department of Applied Physics, California Institute of Technology, Pasadena, CA91125.

ABSTRACT

We describe the performance of submicron microdisk and photonic crystal lasers fabricated within InGaP/InGaAlP quantum well material. The smallest lasers, with diameters of approximately 600 nm, feature ultra-small mode volumes and exhibit single mode operation at low threshold powers. Their small cavity volumes of approximately 0.03 μm^3 for microdisk lasers and 0.01 μm^3 for photonic crystal lasers enable them to be used as spectroscopic sources. Here we demonstrate the fabrication and characterization of visible, monolithically fabricated, submicron mode volume lasers.

Key words: laser, microdisk, photonic crystal, visible, InGaP, InGaAlP, microcavity, nanofabrication, quantum well, spectroscopic source

1. INTRODUCTION

Semiconductor microcavities have been intensively studied because of many reasons including their possibilities of high scale integration, the potential of thresholdless lasing and strong coupling of electron and photon states. In microcavities, microdisks and photonic crystals cavities are two important geometries. Microdisk lasers based on whispering gallery mode cavities have been studied for many years, and were originally pioneered in InGaAsP material emitting in the telecommunication wavelength range. High Q-factors, monolithic fabrication, and the possibility of dense integration make the microdisk geometry a very promising candidate for optical communications and chemical sensing. By selecting various materials systems, microdisk lasers have been demonstrated at many different wavelengths ranging from the UV to the IR.[1-6] By depositing one contact on the top surface of the disk and establishing a conducting path from the laser through the substrate, electrical injection lasers have also been realized in this geometry.[7-9] Shrinking the disk size was shown to enable large scale integration and low energy consumption. However, due to the high optical bend losses inherent to small disk microcavities, much research still focuses on cavity sizes over 2 μm in diameter. The smallest disk laser reported in the literature so far consisted of a 1.6 μm diameter laser fabricated in the InGaAs/InGaAsP quantum well (QW) material system[10] in 1992. In the microdisk section, we report even smaller visible microdisk lasers fabricated in InGaP/InGaAlP QW material and emitting light at a wavelength of approximately 670 nm. The 645 nm diameter of our free standing disk laser is smaller than the vacuum emission wavelength. The cavity volumes of these whispering gallery mode devices, calculated to be approximately 0.03 μm^3, are well suited for the exploration of laser performance at the extreme limits of laser size, operating well into the so-called nano scale regime. Ultra-small lasers in visible light emitting materials systems are also expected to be excellent spectroscopy sources to perform very local chemical and biological measurements.

Compared to microdisk cavities as well as other conventional cavities, photonic crystal cavities offer many advantages for achieving ultrasmall modal volumes while maintaining high quality factors[11-15]. When combining such cavities with light emitting active materials, such as QWs[11] and QDs[13], it is possible to form ultrasmall lasers that can be highly integrated. And each laser cavity supports only very few optical modes. This results in the potential for high frequency modulation of such lasers[16], which made these devices very interesting for applications in optical data communication. So far, most research on photonic crystal lasers has focused on near-infrared wavelength emission using InGaAsP or InGaAs active materials. It has been difficult to obtain small mode volume lasers in visible light emitting

material systems due to high surface carrier recombination velocities or the lack of high refractive index contrast substrates for light confinement in the vertical direction[17-20]. Visible photonic crystal lasers operating in the spectral vicinity of 670nm could enable a broad range of important applications, including high density optical recording, high resolution visible laser projection displays, and, most importantly, compact spectroscopic sources as ultrasmall sensors for biological and chemical detection within small sample volumes. In the photonic crystal section, we present our first experimental results of such a two dimensional photonic crystal slab laser that can satisfy these needs.

2. DESIGN AND FABRICATION

InGaP/InGaAlP quantum wells were grown by metallorganic chemical vapor deposition (MOCVD) on top of a sacrificial AlGaAs layer, deposited onto a GaAs substrate. Optical gain was provided by two 7 nm thick and compressively strained InGaP quantum wells that were separated by 10 nm InGaAlP barriers (Figure 1a). The active quaternary material was designed to emit light at ~670 nm (Figure 1b). Due to the compressively strained quantum wells, light was strongly coupled into transverse electric (TE) modes. The quantum well active material was placed within the center of a 170 nm InGaAlP slab, and 5 nm InGaP lattice matched layers were used on the top and bottom sides of the slab to protect the oxidation of aluminum in the quaternary compound. A 700 nm thick sacrificial AlGaAs layer was introduced between the slab and the GaAs substrate, designed to be removed through a selective chemical etch to avoid coupling losses from the disk wings into the substrate. Following the epitaxial growth of the InGaP/InGaAlP material, the wafers were coated with a 100 nm SiON hard mask and 200 nm Zep520 electron beam resist.

Electron beam lithography was then used to define cavity patterns within the Zep520 electron beam resist. For microdisks, ring patterns were defined (Figure 1c). The inner circles defined the disk diameters and the widths of the rings were designed to prevent optical coupling losses from the disk edge into the surrounding quantum well material. Reactive ion etching (RIE) was subsequently used to directionally transfer the lithographic pattern from that resist into the SiON etch mask by using a CHF$_3$ plasma. After removal of the resist, the hard mask pattern was further transferred through the InGaP active layer with an iodine-based inductively coupled plasma reactive ion etch (ICP-RIE). Time controlled steam oxidation of the AlGaAs by water vapor within a tube furnace followed by the potassium hydroxide (KOH) chemical dissolution of the resulting aluminum oxide formed the mushroom shaped microdisk structure shown in Figure 2. Dilute buffered HF was finally used to remove the SiON etch mask. As an alternative to electron beam lithography, it should also be possible to define the microdisk laser disks by photolithography, which provides the opportunity of high throughput production of ultra-small lasers. By defining a post radius to 0.2 µm smaller than that of the microdisk, we minimize the light leakage through the post while maintaining acceptable heat sinking of the active laser mode volume. We have fabricated and characterized many different sizes of disks, with diameters ranging from 1.6 µm down to 0.5 µm, by deliberately decreasing the diameter in 100 nm steps. In these laser arrays, we observe lasing in all of the disks except for the 0.5 µm diameter devices.
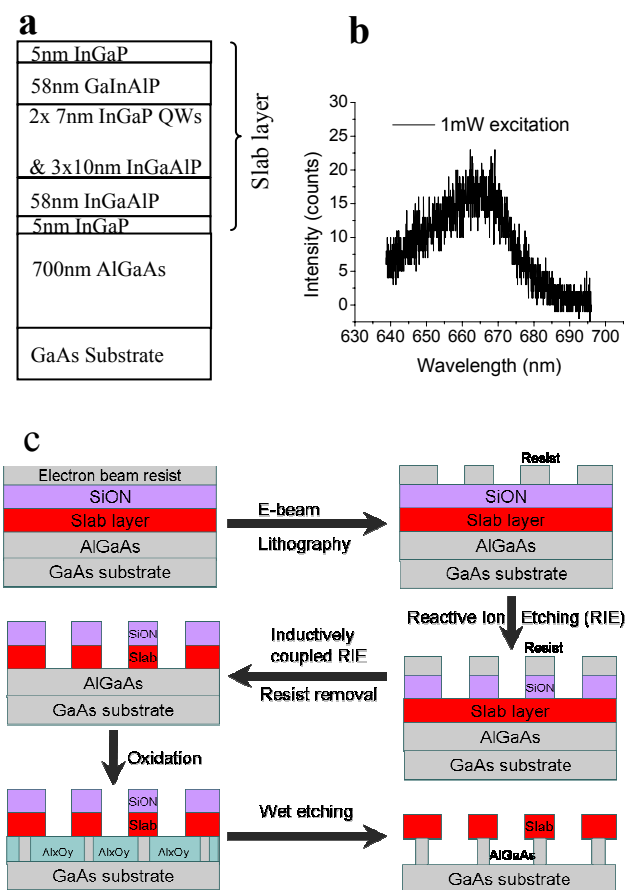

Figure 1. (a) Schematic epitaxial layer sequence of our slab composition and **(b)** a typical photoluminescence emission spectrum taken from the grown wafer. **(c)** The fabrication procedure flow chart.
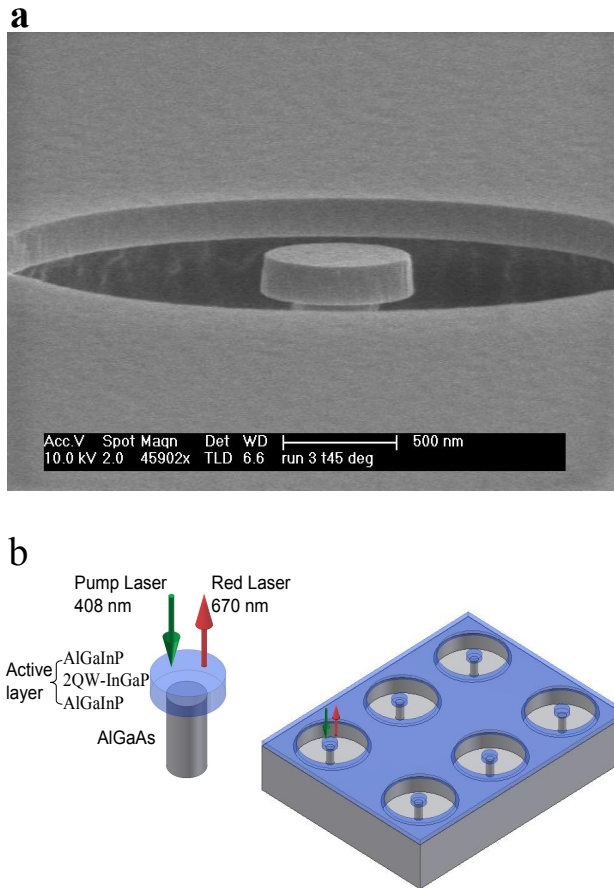
a

b

Figure 2. (a) Scanning electron microscope image of a 0.6 μm diameter submicron microdisk laser structure. **(b)** Illustration of mushroom shape structure and pumping scheme.
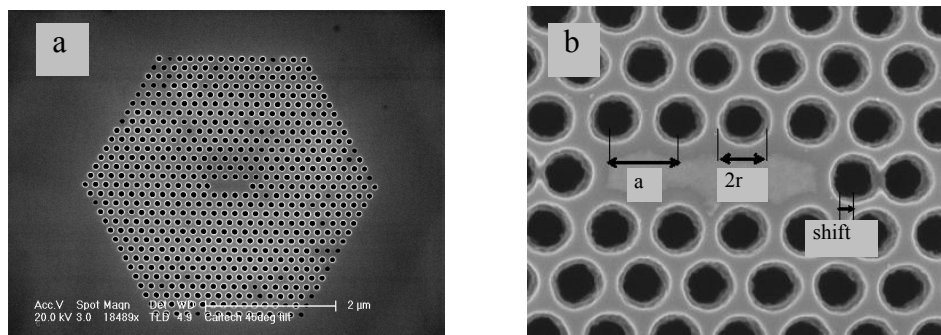
For photonic crystals, we used a high Q cavity design first proposed by Akahane [15] consisting of a L3 linear defect (removing 3 holes) within a triangular photonic crystal lattice of holes on a thin high-index slab. This design reduces the loss in the vertical direction by shifting the holes at the end of the defect area outwards. Figure 3 shows the top view of a fabricated photonic crystal microcavitiy slab. The lattice spacing, a, the radius of hole, r and the shift of the hole were defined as shown in the Figure 3b. We lithographically controlled the ratio between the hole shift and the lattice spacing (shift/a) to be 0.2. Also, we lithographically varied the lattice spacing (a) within a range from 0.14μm to 0.18μm and the ratio between the hole radius and lattice spacing (r/a, the porosity factor) from 0.25 to 0.29. Fourteen periods of photonic crystal lattice (Fig. 3a) were used to surround the defect within the 170nm thick quantum well active layer slab which has a refractive index of around 3.4 at 670nm. The photonic crystal and cavity dimensions were designed to match the 670nm emission wavelength of the InGaP active material. The fabrication process procedure is the same as shown in Figure 1b except that we undercut the space beneath the active layer to form a 2D photonic crystal slab.

3. MEASUREMENT

The microdisks were optically pumped at room temperature using 8 ns pulses separated by 30 μs periods (0.027% duty cycle) with a 407 nm InGaN semiconductor diode laser. The pump beam was focused onto the sample surface, vertically coupling the excitation light (Figure 2 b) through a 50x objective lens to form a pump beam spot size less than 3 μm in diameter. Free space pumping does not require fine alignment of the

Figure 3. Scanning electron microscope image of photonic crystal laser cavity **(a)** low magnification image showing the entire device and **(b)** higher resolution image showing the details of the cavity.

optical fiber to the disk, an advantage especially for the submicron disk sizes described here. Moreover, free space pumping covers the entire disk area and renders the cavity and the central part of the laser disk transparent to minimize

re-absorption in the central disk portion. However, the pumping and collection of laser emission from the disk are not very efficient. In the other hand, the suspended photonic crystal slab cavities were optically pumped at room temperature at the same setup using 5ns pulses at 10 kHz (0.005% duty cycle). The pump beam was focused onto the sample surface to form an excitation beam spot size about 2 μm in diameter. The excitation power used in this paper was determined by dividing the averaged pulse power by the duty cycle. The emission from the lasers was then collected through the same objective lens and lasing spectra were taken with a liquid nitrogen cooled CCD (Princeton instruments, Spec10) detector filtered by a monochromator (Acton, SpectraPro). The monochromator entrance slit width was set to a width of 10 μm and a 1200 g/mm grating was used, resulting in a spectral resolution of approximately 0.1 nm. An additional flip-up mirror was used to guide the light into a CCD imaging system to view images of laser cavity modes as well as the excitation pump spot.

4. MICRODISKS

Figure 2a shows an angled view of a completely fabricated ultrasmall microdisk, taken in a scanning electron microscope (SEM). The sidewall roughness of the disk is less than 20 nm and the non-vertical sidewall is due to the
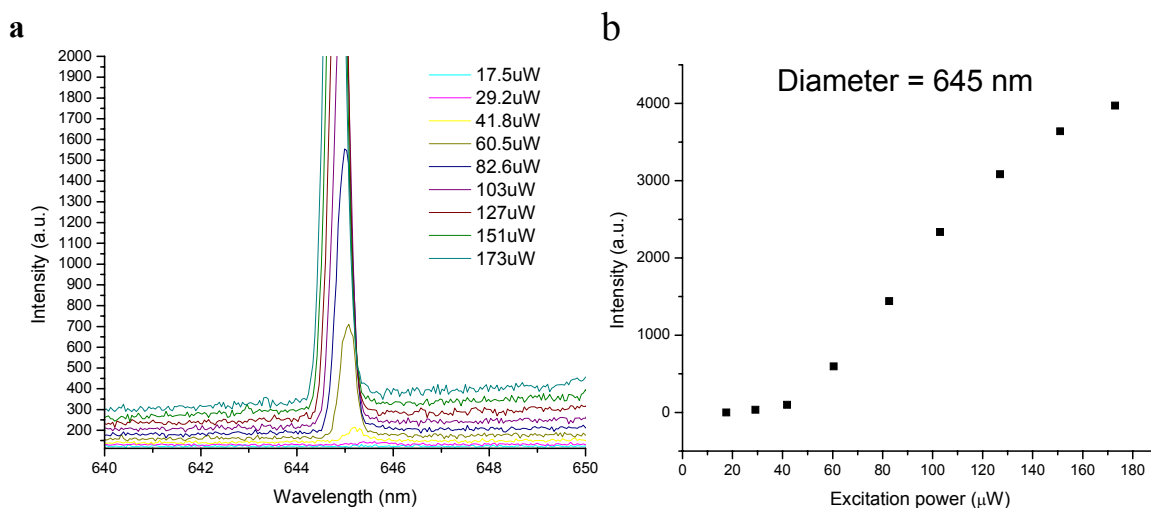
Figure 4. (a) The Spectra with different excitation power and **(b)** L-L curve of one of the 645 nm diameter microdisks.

non-optimized dry etching recipe which could be further improved. Figure 2b illustrates the excitation and detection scheme used in this experiment, and it should be noted that this free space pump - collection measurement scheme is not efficient since a large portion of the excitation light does not couple into the mode. Indeed, much of the emitted light also escapes horizontally along the disk plane and vertically into the GaAs substrate. We expect that much higher output power and lower thresholds can be observed when using fiber-coupling measurements. Figure 4 shows luminescence spectra and an L (excitation power)-L (lasing peak intensity) curve from a device with disk diameter 645 nm and post diameter 200 nm. The laser threshold was measured to be approximately 50 μW. This threshold power is similar to that of photonic crystal slab lasers that we recently fabricated within the same InGaP material system. Above 120 μW, heating of the laser cavity ultimately limits the output power, and the L-L curve saturates. Figure 5 shows the lasing characteristics of another ultrasmall microdisk with disk diameter 650 nm and post diameter 350 nm. The laser threshold was measured to be approximately 187 μW and saturation occurred when the power exceeded 250 μW. Both cavities exhibited distinct threshold behavior with linear L-L response of the output power above threshold and before saturation. Figure 5 also shows the semi-logarithmic plot of the L-L curve, confirming the lasing characteristics. The difference in threshold and saturation powers in the two smallest lasers may be due to the larger size post of the 650 nm disk. In both cases, we observed a blue shift of the emission as the excitation power increases. This is due to an increase of effective refractive index which is approximately proportional to the increase in carrier density. Figure 6 shows spectra of some other lasers.
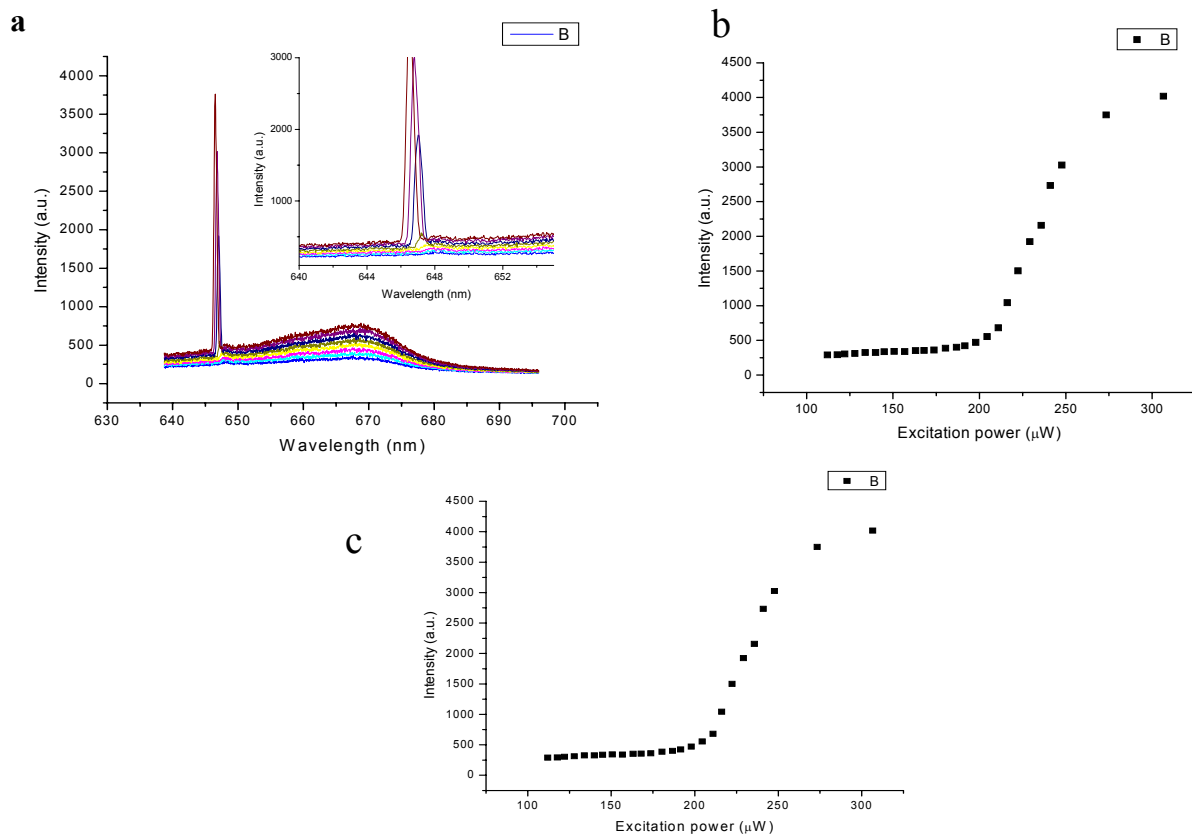
Figure 5. (a) The Spectra with different excitation powers and **(b)(c)** Linear and semi-logarithmic plot of L-L curve of a 650 nm diameter microdisks.
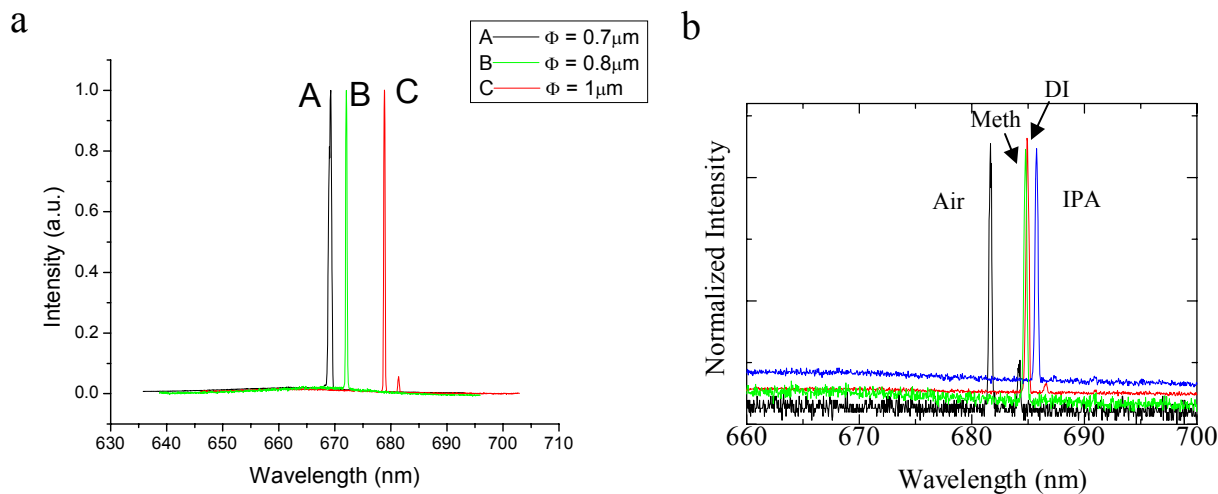

Figure 6. (a) Laser spectra with different diameter microdisks and **(b)** Lasing peak wavelength shift obtained with different chemical environments. Black line denotes spectrum in air; green denotes spectrum in methanol; red denotes spectrum in DI water and blue denotes the spectrum in IPA.

Single mode operation was maintained until the disk diameter was increased to 1 μm. The small peak on the right of the 1 μm disk main peak may be a result of propagation direction degeneracy, caused by nonsymmetrical, or random roughness from the fabrication process.

The use of microdisk lasers for spectroscopic analysis has been described earlier.[21] Here we use the ultrasmall mode volume microdisk lasers to provide more sensitivity to the environmental refractive index changes and molecules attached onto the disk surface. Figure 6 shows the spectra of a 1 μm diameter disk when used as a refractive index monitor.
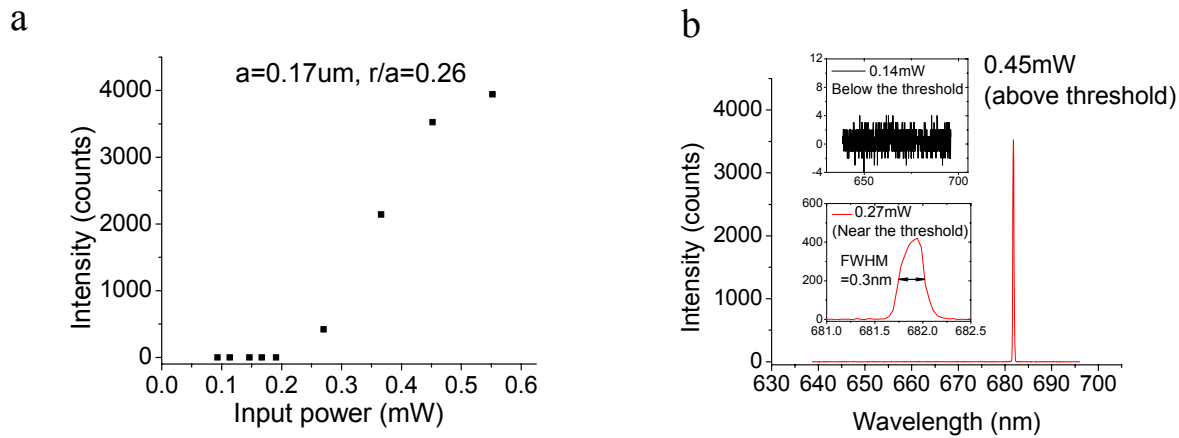

Figure 7. (a) L-L curve **(b)** Typical lasing spectrum of an InGaP 2D photonic crystal laser with a lattice parameter of a=0.17μm and porosity factor r/a=0.26.

The lasing peak shifts from 681.6 nm to 684.8 nm when the disk is surrounded by methanol, to 684.9 nm when in deionized water, and to 685.8 nm when immersed in iso-propyl alcohol (IPA). The sensitivity of the microdisk is ~0.09 in refractive index per nanometer wavelength shift. We expect higher sensitivities in even smaller disks since the optical
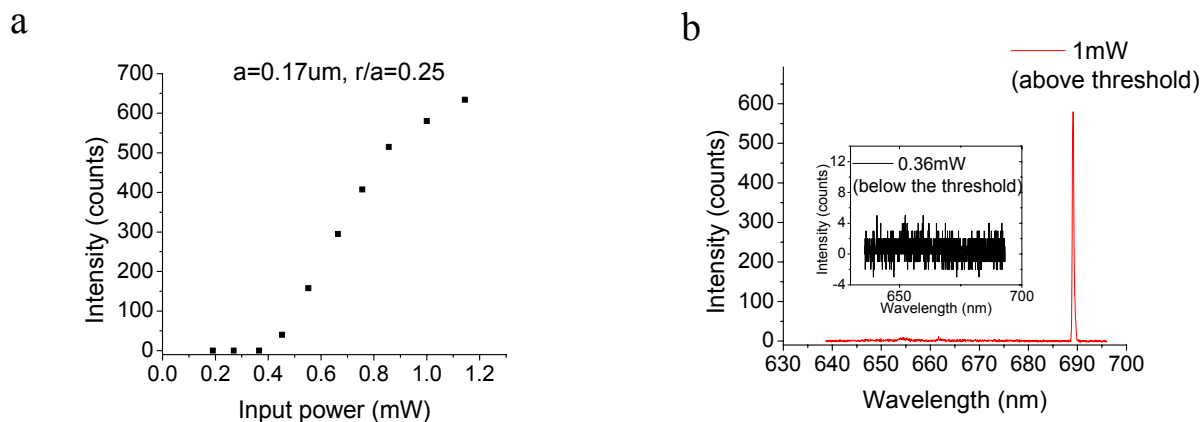

Figure 8. (a) L-L curve **(b)**Typical lasing spectrum for an InGaP 2D photonic crystal laser with a lattrice parameter of a=0.17μm and a porosity factor r/a=0.25.

mode is more extended to the outside of the disk, and mode hopping can be avoided by utilizing disks that support only few modes.

5. PHOTONIC CRYSTALS

Figure 7 shows luminescence spectra and the L(excitation power)-L(lasing peak intensity) curve from a device with lattice parameter a=170nm and porosity factor r/a=0.26. The laser threshold was determined to be approximately 250μW, and the linewidth was measured as 0.3nm at threshold, yielding an effective Q of about 2000. Below threshold,

only a broad background from the gain medium was measured from this cavity. Above 450µW, heating of the laser cavity limited the output power, and the L-L curve saturated. The 2D photonic crystal cavity peak can be tuned by changing either the porosity or the lattice parameter of the photonic crystal lattice surrounding the nanocavity. Figure 8 shows a laser with a slightly lower porosity (porosity factor r/a=0.25). For this laser, the measured laser threshold was 400µW, and the device again saturated as a result of cavity heating above 1mW. Both cavities exhibited distinct threshold and linearity in the output power above threshold but before saturation. The lasing characteristic was very sensitive to the position of the excitation beam spot (~1µm movement), which indicates that lasing occurs from a localized defect mode.

Figure 9a shows the influence of changing of the porosity on the laser emission wavelength, whereas Figure 9b shows a similar tuning curve for changes in the photonic crystal lattice parameter. The uneven spectral shifts result from
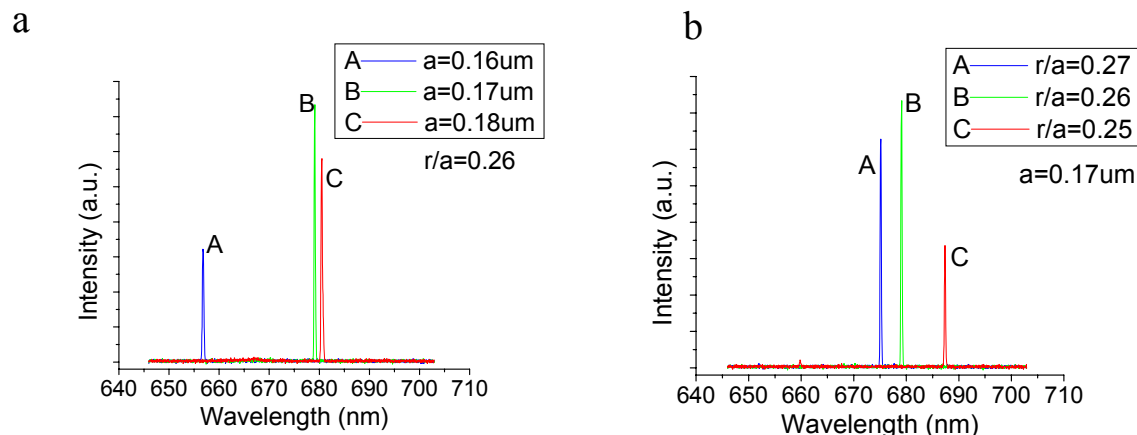

Figure 9. (a) r/a fixed to 0.26 **(b)** Lattice spacing fixed to 0.17µm (the uneven spectral shifts result from fabrication variation and device scaling only in two dimensions due to the fixed slab thickness).

fabrication variation and device scaling only in two rather than three dimensions due to the fixed slab thickness. This data indicates that the InGaP photonic crystal lasers can be lithographically tuned throughout the gain emission of the quantum wells. The accuracy of such tuning is only limited by the quality and reproducibility of the fabrication process. It should be noted that the minimum feature size required for the successful definition of the photonic crystal mirror surrounding the laser cavities is approximately 30nm, which is the distance between two adjacent holes in the slab. Compared to conventional InGaAsP material systems operating at 1550nm, our fabrication process has to overcome the feature size scaling associated with the 2.3 times decreases in wavelength. Nevertheless, with our fabrication approach, it is possible to define dense arrays of laser cavities that are separated by as little as 2 microns. Compact multi-spectral sources can therefore be defined within the visible wavelength range.

6. SUMMARY:

In summary, we have fabricated ultrasmall disk lasers with optical mode volume of only 0.03 µm^3 in InGaP QW material. We achieved excitation threshold as low as 50 µW in the 645 nm disk. We also showed the lasing spectra from different diameter submicron microdisks and demonstrate the use of these ultrasmall disk lasers for refractive index monitoring. In the other hand, we fabricated the visible 2D photonic crystal slab lasers. The use of photonic crystal lasers for spectroscopic analysis has been described earlier[22], and offers the opportunity to define ultra-small optical cavities with enormous optical field intensities. These devices have been used in the past as refractive index sensors, indicating the refractive index of volumes as small as 10^{-17} liters, limited by the mode volume of 0.03 cubic microns at 1550nm wavelength. In our experiments, we have defined lasers within a wavelength range that is even more interesting for spectroscopic applications, as many of the fluorophores used for biological analysis are limited to the visible spectrum, and single-photon detectors are available at such wavelengths. Moreover, these devices may become very interesting sources for Raman spectroscopy and other specific measurements of the chemical composition of the femtoliter contents of an optical nanocavity. We expect InGaP lasers to be very useful for biochemical analysis as well as for efficient displays and high-frequency lasers in the near future.

ACKNOWLEDGEMENTS

REFERENCES

(1) S. L. Mccall; A. F. J. Levi; R. E. Slusher; S. J. Pearton; R. A. Logan, "Whispering-Gallery Mode Microdisk Lasers", Applied Physics Letters, **60(3)**, 289-291, 1992.

(2) U. Mohideen; W. S. Hobson; S. J. Pearton; F. Ren; R. E. Slusher, "Gaas/Algaas Microdisk Lasers", Applied Physics Letters, **64 (15)**, 1911-1913, 1994.

(3) J. S. Pan; P. H. Cheng; T. D. Lee; Y. C. Lai; K. C. Tai, "0.66 μm InGaP/InGaAlP single quantum well microdisk lasers", Japanese Journal of Applied Physics Part 2-Letters, **37,(6A)**, L643-L645, 1998.

(4) M. Hovinen; J. Ding; A. V. Nurmikko; D. C. Grillo; J. Han; L. He; R. L. Gunshor, "Blue-Green Laser-Emission from Znse Quantum-Well Microresonators", Applied Physics Letters, **63 (23)**, 3128-3130, 1993.

(5) S. S. Chang; N. B. Rex; R. K. Chang; G. Chong; L. J. Guido, "Stimulated emission and lasing in whispering-gallery modes of GaN microdisk cavities", Applied Physics Letters, **75(2)**, 166-168, 1999.

(6) P. Michler; A. Kiraz; C. Becher; W. V. Schoenfeld; P. M. Petroff; L. D. Zhang; E. Hu; A. Imamoglu, "A quantum dot single-photon turnstile device", Science, **290 (5500)**, 2282-2285, 2000.

(7) A. F. J. Levi; R. E. Slusher; S. L. Mccall; T. Tanbunek; D. L. Coblentz; S. J. Pearton, "Room-Temperature Operation of Microdisk Lasers with Submilliamp Threshold Current", Electronics Letters, **28 (11)**, 1010-1012, 1992.

(8) T. Baba; M. Fujita; A. Sakai; M. Kihara; R. Watanabe, "Lasing characteristics of GaInAsP-InP strained quantum-well microdisk injection lasers with diameter of 2-10 μm", Ieee Photonics Technology Letters, **9 (7)**, 878-880, 1997.

(9) L. D. Zhang; E. Hu, "Lasing emission of InGaAs quantum dot microdisk diodes", Ieee Photonics Technology Letters, **16 (1)**, 6-8, 2004.

(10) A. F. J. Levi; S. L. Mccall; S. J. Pearton; R. A. Logan, "Room-Temperature Operation of Submicrometer Radius Disk Laser", Electronics Letters, **29 (18)**, 1666-1668, 1993.

(11) O. Painter, R. K. Lee, A. Scherer, A. Yariv, J. D. O'Brien, P. D. Dapkus, and I. Kim, "Two-dimensional photonic band-gap defect mode laser", Science **284 (5421)**, 1819-1821, 1999.

(12) M. Loncar, T. Yoshie, A. Scherer, P. Gogna, and Y. M. Qiu, "Low-threshold photonic crystal laser", Appl Phys Lett **81 (15)**, 2680-2682 2002.

(13) T. Yoshie, O. B. Shchekin, H. Chen, D. G. Deppe, and A. Scherer, "Quantum dot photonic crystal lasers", Electron Lett **38 (17)**, 967-968 2002.

(14) K. J. Vahala, "Optical microcavities", Nature **424 (6950)**, 839-846 2003.

(15) Y. Akahane, T. Asano, B. S. Song, and S. Noda, "High-Q photonic nanocavity in a two-dimensional photonic crystal", Nature **425 (6961)**, 944-947 2003.

(16) T. Yoshie, M. Loncar, A. Scherer, and Y. Qiu, "High frequency oscillation in photonic crystal nanolasers", Appl Phys Lett **84 (18)**, 3543-3545 2004.

(17) M. Campbell, D. N. Sharp, M. T. Harrison, R. G. Denning, and A. J. Turberfield, "Fabrication of photonic crystals for the visible spectrum by holographic lithography", Nature **404 (6773)**, 53-56 2000.

(18) X. Wu, A. Yamilov, X. Liu, S. Li, V. P. Dravid, R. P. H. Chang, and H. Cao, "Ultraviolet photonic crystal laser", Appl Phys Lett **85 (17)**, 3657-3659 2004.

(19) Y. S. Choi, K. Hennessy, R. Sharma, E. Haberer, Y. Gao, S. P. DenBaars, S. Nakamura, E. L. Hu, and C. Meier, "GaN blue photonic crystal membrane nanocavities", Appl Phys Lett **87 (24)**, 2005.

(20) C. Meier, K. Hennessy, E. D. Haberer, R. Sharma, Y. S. Choi, K. McGroddy, S. Keller, S. P. DenBaars, S. Nakamura, and E. L. Hu, "Visible resonant modes in GaN-based photonic crystal membrane cavities", Appl

Phys Lett **88 (3)**, 2006.

(21) W. Fang; D. B. Buchholz; R. C. Bailey; J. T. Hupp; R. P. H. Chang; H. Cao, "Detection of chemical species using ultraviolet microdisk lasers", Applied Physics Letters**, 85 (17)**, 3666-3668, 2004.

(22) M. Loncar, A. Scherer, and Y. M. Qiu, "Photonic crystal laser sources for chemical detection", Appl Phys Lett **82 (26)**, 4648-4650, 2003.